PHYSICAL REVIEW B **83**, 115409 (2011)

Computational prediction of L_3 EXAFS spectra of gold nanoparticles from classical molecular dynamics simulations

Otello Maria Roscioni,[1,2] Nicholas Zonias,[2] Stephen W. T. Price,[2] Andrea E. Russell,[2] Tatiana Comaschi,[3] and Chris-Kriton Skylaris[2,*]

[1]*Dipartimento di Chimica Fisica e Inorganica, Università di Bologna, viale Risorgimento 4, IT-40136 Bologna, Italy*
[2]*School of Chemistry, University of Southampton, Highfield, Southampton SO17 1BJ, United Kingdom*
[3]*Dipartimento di Fisica "E. Amaldi," Università di Roma Tre, via della Vasca Navale 84, IT-00146 Roma, Italy*

(Received 12 November 2010; published 8 March 2011)

We present a computational approach for the simulation of extended x-ray absorption fine structure (EXAFS) spectra of nanoparticles directly from molecular dynamics simulations without fitting any of the structural parameters of the nanoparticle to experimental data. The calculation consists of two stages. First, a molecular dynamics simulation of the nanoparticle is performed and then the EXAFS spectrum is computed from "snapshots" of structures extracted from the simulation. A probability distribution function approach calculated directly from the molecular dynamics simulations is used to ensure a balanced sampling of photoabsorbing atoms and their surrounding scattering atoms while keeping the number of EXAFS calculations that need to be performed to a manageable level. The average spectrum from all configurations and photoabsorbing atoms is computed as an Au L_3-edge EXAFS spectrum with the FEFF 8.4 package, which includes the self-consistent calculation of atomic potentials. We validate and apply this approach in simulations of EXAFS spectra of gold nanoparticles with sizes between 20 and 60 Å. We investigate the effect of size, structural anisotropy, and thermal motion on the gold nanoparticle EXAFS spectra and we find that our simulations closely reproduce the experimentally determined spectra.

DOI: 10.1103/PhysRevB.83.115409 PACS number(s): 61.05.cj, 61.46.Df, 61.46.Hk, 34.20.Cf

I. INTRODUCTION

Small metal nanoparticles, with diameters in the range of 1–10 nm, present some fascinating physical and chemical properties when compared to their bulk counterparts. These can be attributed to the discretization of their energy levels, which are strongly dependent on their morphology.[1,2] Therefore, their electronic, magnetic, and optical properties are "tunable" with the size, shape, and surface termination of the nanoparticle and, as a result, make them attractive for applications in catalysis, biosensing, and electronic devices.

It is important to have reliable synthetic pathways to be able to obtain metal nanoparticles that are uniform and of the desirable chemical and physical properties. Equally important for this goal is the ability to characterize the produced nanoparticles in order to ascertain that the desired morphology has been produced. The x-ray diffraction technique (XRD) can provide very precise structure determination in the case of molecular crystals, but, in the case of the metallic nanoparticles, it can result in significant ambiguity in attempts to accurately measure cell parameters and atomic distances. On the other hand, x-ray absorption spectroscopy (XAS), and more specifically within the extended x-ray absorption fine structure (EXAFS) region, has been able to provide accurate results for the atomic structure of nanoparticles as a function of temperature.[3,4] Within this framework, factors that can induce structural reconstructions, such as surface tension, capping ligands, steric hindrance effects, and metastable states, can significantly alter their physicochemical properties and can be quantified by EXAFS experiments.[5]

In this paper, the effects of structural anisotropy and thermal motions on the EXAFS spectrum of gold nanoparticles with sizes between 20 and 60 Å have been investigated. These effects have been addressed by carrying out multiple-scattering (MS) calculations of XAS spectra. Contrary to the norm of fitting the structural parameters of the simulated system to match the experimental data, here we follow a first-principles approach where our spectra are computed directly from molecular dynamics simulations without carrying any parametrizations.

The gold nanostructures studied in this work are representative structures of the gold nanoparticles synthesized by Comaschi *et al.*[6] These directly refer to the Au L_3-edge XAS data of two noncoated gold nanoparticles with experimentally reported mean diameters of 50 ± 7 Å (Au-NP1) and 24 ± 8 Å (Au-NP4). The latter nanoparticle samples were either prepared by using the solvated atom dispersion (SMAD) technique or produced under vacuum on a very thin polymer film by consecutive evaporation of gold and Mylar, respectively. The SMAD technique[6–8] involves (i) deposition of an organic solvent on the reactor walls cooled down to very low temperatures, (ii) vaporization of the metal under vacuum and then rapid trapping in a frozen solvent, (iii) warming up at room temperature of the solvated atoms, and (iv) impregnation to a surface of amorphous silica and drying of the samples at room temperature. The gold nanoparticles obtained with this method are noncoated and, therefore, their x-ray absorption spectra depend only on their morphology and size.

The XAS measurements were carried out at the BM08 GILDA beamline of the ESRF in Grenoble (France). The spectra were recorded at the L_3 edge of Au in transmission mode. The sample temperature was varied from 20 up to 300 K using a liquid-helium cryostat, with the sample immersed in a He gas atmosphere.

We have constructed models of gold nanoparticles that correspond to the experimentally determined diameters and have observed their dynamic behavior and structures at various temperatures by performing classical molecular dynamics

(MD) simulations. Such simulations are often used to study the dynamical behavior of nanoparticles, even in conditions far from ambient such as, for example, under high external pressure.[9] Our simulations have been performed with a force field that was designed to reproduce the properties of several bulk, metallic systems. Details regarding the parameters and the form of the potential used in the MD simulations are given in Sec. II.

The information extracted from the MD simulations can be used to perform a quantitative analysis of XAS data, as has been successfully applied so far to disordered systems, such as aqueous solutions of ions.[10–16] It has also been shown that the damping of the XAS signal associated with the structural disorder, which is expressed normally through the Debye-Waller factor, can be reproduced through the average of XAS spectra computed from a statistically representative number of computer-generated configurations ("configurational average").[11]

In calculating the XAS spectrum of a nanoparticle, asymmetry effects due to the finite size of the nanoparticles, which increase as the nanoparticle size decreases, have to be taken into account. Thus, we have assumed that every atom inside the nanoparticle can give rise to absorption and, therefore, the resulting XAS spectrum should include the contributions of atoms in different atomic environments. This is achieved by sampling several absorption sites in different positions, starting from the center of mass of the nanoparticle and ending at the nanoparticle's surface. Since several atoms share an equivalent atomic environment, they are grouped into shells, which, in this case, are defined by the distance from center of mass of the nanoparticle. The details regarding the choice of the absorption sites are analyzed and discussed in Secs. III and IV, along with a brief description of the MD trajectory production.

II. COMPUTATIONAL PROCEDURE

A. The Gupta potential

The interactions between the Au atoms in our MD simulations are described by the Gupta classical force field.[17] The Gupta potential is a semiempirical potential used to describe the interatomic interactions of metallic systems and is derived from fitting experimental data into an assumed functional form. It is based on the second moment approximation of tight-binding theory and has been extracted from Gupta's expression for the cohesive energy of a bulk material. The potential is divided into a repulsive (V^r) and many-body attractive terms (V^m) summed over all atoms (N) contained in the molecular system:

$$V_{\text{clus}}(\mathbf{r}_1,\mathbf{r}_2,\ldots,\mathbf{r}_N) = \sum_{i=1}^{N}\{V^r(\mathbf{r}_i) - V^m(\mathbf{r}_i)\}, \qquad (1)$$

where

$$V^r(\mathbf{r}_i) = \sum_{j\neq i}^{N} A\exp\left[-p\left(\frac{r_{ij}}{r_0}-1\right)\right] \qquad (2)$$

and

$$V^m(\mathbf{r}_i) = \left\{\sum_{j\neq i}^{N}\zeta^2\exp\left[-2q\left(\frac{r_{ij}}{r_0}-1\right)\right]\right\}^{\frac{1}{2}}, \qquad (3)$$

where r_{ij} is the distance between atoms i and j, A is the energy scaling factor for the repulsive energy, ζ is the energy scaling factor for the many-body attractive energy, r_0 is the equilibrium bond length of the bulk material, and p and q are the range exponents for the pair and many-body potentials, respectively. The potential parameters A, ζ, p, and q are usually fitted to experimental data in order to represent the properties of bulk metals and alloys.

The values of the parameters used in the Gupta force field to describe the interactions between gold atoms are taken from the work of Cleri and Rosato,[18] who performed tight-binding (TB) calculations on several transition metals in order to reproduce the cohesive energy, atomic volume, and elastic constants of the corresponding metallic systems at zero temperature.

B. Molecular dynamics simulations

To obtain realistic ensembles of nanoparticle structures, we have performed classical MD simulations with the DL_POLY2 software package.[19] Our simulations were carried out within the microcanonical (NVE) ensemble, with an integration time step of 1 fs. The atomic forces and velocities were equilibrated for a period of 50 ps after which a production calculation of 2 ns followed. Data were collected during the production stage after confirming that both the energy and temperature were stabilized.

The simulations were performed on Au_{429} and Au_{3925} nanoparticles with average diameters of 24 and 50 Å, respectively, which correspond to the experimentally determined diameters of the nanoparticles. We have additionally performed MD simulations on the Au_{249} (20 Å diameter), Au_{887} (30 Å diameter), and Au_{6699} (60 Å diameter) nanoparticles. These nanoparticles were used for testing size effects and verifying our results. The initial structures for the simulated nanoparticles were constructed with Accelrys Materials Studio.[20] The lattice parameters for constructing the nanoparticles were obtained from a unit-cell representation of the face-centered-cubic (fcc) structure of bulk gold. The unit cell was expanded periodically along each lattice vector and then truncated to form a spherical particle of a specified diameter. Each nanoparticle structure was then relaxed with the Gupta potential. The MD simulations were conducted at temperatures ranging from 20 to 300 K.

For the lowest temperature simulations (20 K), the classical molecular dynamics ensemble is not entirely appropriate as the atomic motion is expected to be mainly due to phonons, in the form of normal mode vibrations of the nanoparticles, which are populated according to Bose-Einstein quantum statistics. However, we have observed that, even in this case, our simulations, to a great extent, agree with the experimental spectra. This is not completely unexpected as the large atomic weight of Au combined with the compact shape of our nanoparticles should lead to phonons with small average quantum vibrational amplitudes. This is also what we observe for the atomic displacements in our classical simulations at this temperature range as a result of the reliable representation of the Au potential energy surface by the Gupta potential.[21]

C. EXAFS calculations

To calculate the EXAFS spectrum for a gold nanoparticle from MD simulations, an XAS quantitative analysis code has been developed. The algorithm on which the code is based is summarized in the flowchart of Fig. 1. The program extracts all the required information from a MD trajectory by reading the coordinates of a gold nanoparticle from each of a fixed set of MD "snapshots." For each snapshot, several absorption sites at different positions inside the nanoparticle are sampled and an EXAFS spectrum is computed. The calculated XAS data are then averaged together to give a mean spectrum. The procedure is iterated by increasing the number of MD snapshots sampled until convergence in the resulting XAS spectrum has been achieved.

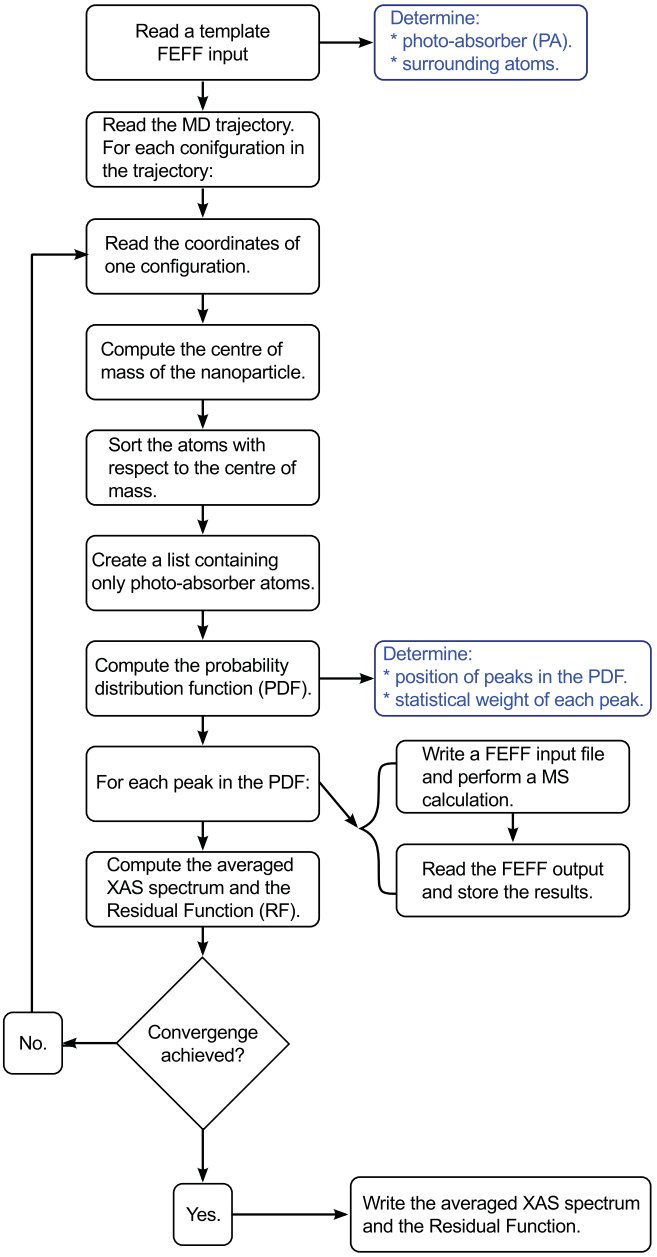

FIG. 1. (Color online) Flow chart of the algorithm used to compute the configurational average of XAS spectra using the structural information derived from MD simulations.

Each mean XAS spectrum is obtained by taking a large number of MD configurations into account. For each configuration, the atoms of the nanoparticle were grouped into "shells" with respect to their distance from the center of mass. For each shell, a photoabsorbing atom was arbitrarily chosen to represent the absorption behavior of the Au atoms inside that shell and to contribute to the XAS spectrum from this region for this particular snapshot (configuration).[11] The atomic shells are defined by using a probability distribution function (PDF), which is obtained as the sum of Gaussian functions centered on each atom of the nanoparticle. The statistical weight of each peak i in the PDF is proportional to the number of photoabsorbing atoms whose distance r_j from the nanoparticle's center of mass satisfies the conditions

$$r_j \geqslant p_i + \Delta_i^+,$$
$$r_j < p_i - \Delta_i^-,$$

where p_i is the position of the peak i in the PDF, $\Delta_i^+ = (p_{i+1} - p_i)/2$ is the distance between the peaks i and $i+1$, and $\Delta_i^- = (p_i - p_{i-1})/2$ is the distance between the peaks i and $i-1$. Therefore, each peak (and the corresponding absorption site) will have a statistical weight proportional to the number of atoms sharing the same physical environment. An example of the PDF generated for a gold nanoparticle structure of 20 Å diameter, including sketches of the corresponding absorbing atoms, is shown in Fig. 2. The accuracy of the PDF depends on the standard deviation of the Gaussian functions and can be tuned accordingly to control the number of peaks in the PDF and, therefore, the number of locations of absorbing atoms being selected (Fig. 3).

The Au L_3-edge EXAFS spectra were computed with the FEFF 8.4 program[22,23] using the Hedin-Lundqvist model of the exchange potential. Atoms up to 10 Å from the photoabsorbing atom were included to obtain converged XAS spectra. In agreement with the data analysis performed previously by

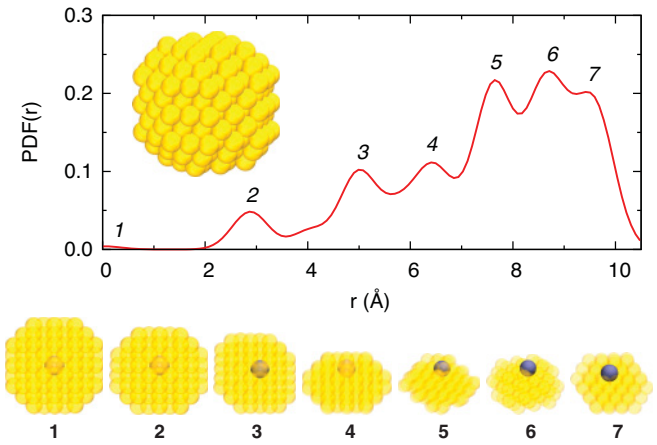

FIG. 2. (Color online) Probability distribution function (PDF) computed for a gold nanoparticle with a diameter of 20 Å. The PDF is proportional to the number of atoms found at a given distance from the center of mass of the nanoparticle. The bottom panel shows the input structures for XAS calculations obtained by applying a cutoff radius of 10 Å around gold atoms chosen from within each shell defined by the peaks of the PDF. The photoabsorbing gold atoms are shown in dark blue, while the gold atoms that define the scattering region are translucent yellow.

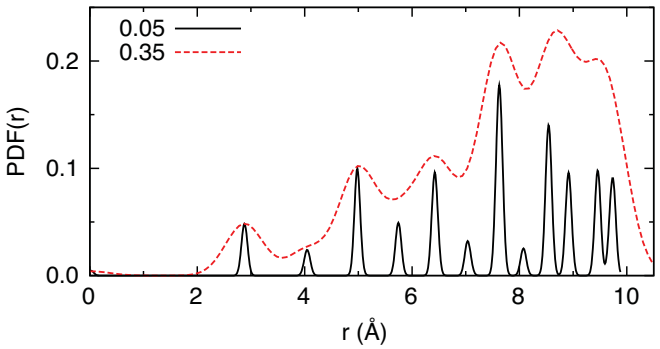

FIG. 3. (Color online) Comparison between the PDF computed for a gold nanoparticle with a diameter of 20 Å using standard deviations of 0.05 (solid line) and 0.35 Å (dotted line). A small standard deviation value results in a fine sampling of atomic shells within the nanoparticle and, as a consequence, a higher number of locations of absorbing atoms being selected.

Comaschi *et al.*,[6] the amplitude reduction factor S_0^2 was set to 0.9, the energy shift was set to 7.1 eV, and the experimental broadening factor was set to 1.0 eV. By applying these settings, the computed Fermi energy for Au nanoparticles was found to be around 7.3 below the L_3 edge of bulk Au (11 919 eV). The Debye-Waller factor has not been taken into account in the calculation, as the thermal damping of the signal is reproduced explicitly through the averaging of the XAS spectra over the nanoparticle configurations.

The number of configurations required to obtain a statistically representative averaged spectrum is determined by calculating a residual function (RF), which is the root mean square of the differences between all the energy points of the averaged XAS spectra computed over $N-1$ and N configurations.[11] An XAS spectrum is considered converged when the corresponding RF value falls below the threshold of 10^{-4} and remains below this value for the following 10 iterations. For gold nanoparticles, about 50 configurations are necessary to achieve convergence of the EXAFS spectra.

III. RESULTS

To validate our approach, we have investigated the dependence of the calculated EXAFS spectrum from several factors and parameters that can affect the XAS calculations. One such factor is the resolution of the PDF. For this, we have studied the dependence of the computed mean Au L_3-edge EXAFS spectrum on the number of absorption environments for a gold nanoparticle with a diameter of 20 Å at 20 K. This choice was made after observing that smaller nanoparticles are affected more strongly by asymmetry effects compared to their larger counterparts. Mean EXAFS spectra for this nanoparticle were computed using PDFs with standard deviations of 0.05 and 0.35 Å, corresponding to a fine and a coarse sampling of absorption sites, respectively. The first case yielded a PDF with 13 different atomic shells, while the second case exposed 7 atomic shells, as shown in Fig. 3. The resulting mean EXAFS spectra and their Fourier transforms (FT) for both cases are shown and compared in Fig. 4. Comparing the two sampling methods, we can observe that the mean spectrum computed with the coarse sampling of the absorption

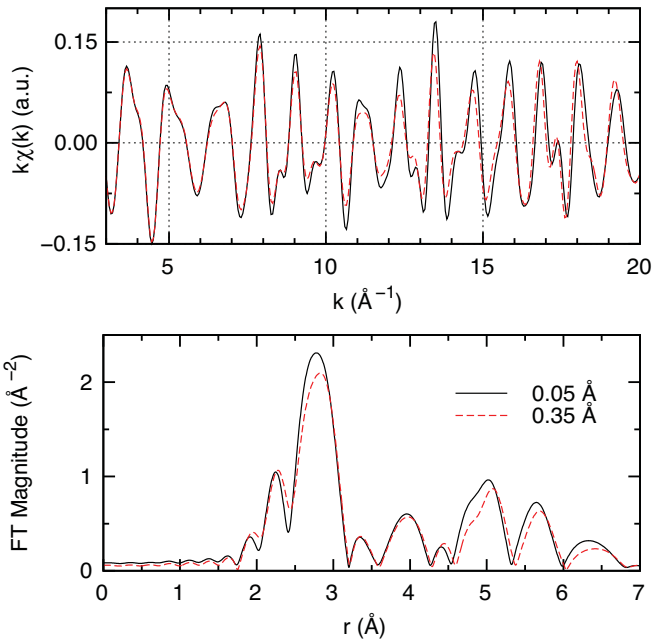

FIG. 4. (Color online) Comparison between the simulated EXAFS spectra and the corresponding Fourier transforms of a gold nanoparticle with a diameter of 20 Å at 20 K. The spectra were computed using a fine sampling (solid line) and a coarse sampling (dotted line) of the photoabsorbing sites through PDF standard deviations of 0.05 and 0.35 Å, respectively.

environments shows a phase shift in the EXAFS signal and a displacement of the peaks toward larger bond distances in the corresponding FT, with respect to the more accurate case of the fine sampling. This result suggests that the contribution of the atomic environments with short Au–Au bond lengths is underestimated in the final spectrum. Indeed, the PDF computed with a coarse sampling, as shown in Fig. 3, does not include the contribution of the outer shell at 9.7 Å, which is present in the PDF computed with a fine sampling and has a statistical weight of 9.5%. As the surface atoms form shorter bond lengths compared to the neighbor pair distances in the core, a poor sampling of the nanoparticle's outer shell underestimates their contribution in the mean EXAFS spectrum and results in the observed phase shift between the spectra computed with a coarse and a fine sampling of the absorption sites. This behavior is consistent with the experimental observation of atomic surface contraction in gold nanocrystals.[24] For this purpose, we have directly investigated the surface compression in our nanocrystals by measuring the nearest-neighbor distances of Au atoms as a function of their distance from the center of mass in order to quantify the effects of the surface tension.[25] A diagram of the resulting bond-length distributions, averaged over all the snapshots, is shown in Fig. 5. All nanoparticles display a clear shortening of the Au–Au bond length as we move from the nanoparticle's core toward the surface, where it reaches a minimum value. Therefore, the different phases of the mean EXAFS spectra originate from the contribution of surface atoms and account for 9.5% in the final spectrum.

Another parameter being investigated is the dependence of the spectra on the nanoparticle size. It is desirable to

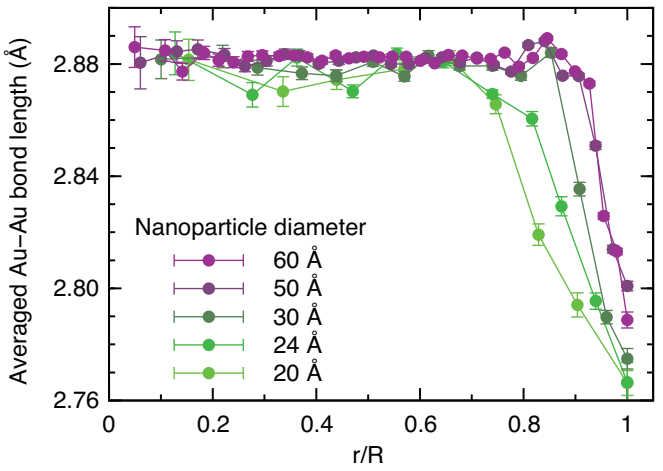

FIG. 5. (Color online) Au–Au bond lengths distribution, averaged over MD snapshots, as a function of the distance from the nanoparticle's core.

be able to use EXAFS spectra to determine the size of the nanoparticles being measured. We have therefore studied several gold nanoparticles with diameters ranging from 20 to 60 Å. The resulting spectra, shown in Fig. 6, reveal that the intensity of EXAFS oscillations increases with the size of the nanoparticle. No shift was observed in the phase of EXAFS oscillations, in contrast to the reported shift between the experimentally obtained EXAFS spectra of Au nanoparticles with mean diameters of 50 and 24 Å. The latter can give rise to a difference of 1% between the best fit of Au–Au bond lengths.[6] However, the radial distribution functions (RDFs) derived from the MD trajectories and shown in Fig. 7 demonstrate that the shape of the peaks in a small nanoparticle is strongly asymmetric and very sensitive to its size, when compared with bulk gold. Furthermore, the position of the peaks is displaced toward smaller values than those of the bulk phase as a result of the contribution from surface atoms. These effects decrease rapidly with respect to the nanoparticle size; for a nanoparticle with a diameter of 60 Å, the peaks of the RDF are barely distinguishable from the peaks of the bulk phase. Hence, for a nanoparticle of this size, the region influenced by the surface tension can account approximately for 20% of its volume (Fig. 5), while for a nanoparticle with a diameter of 20 Å, the same region accounts roughly for 64% of the nanoparticle's volume. (For this estimate, we have approximated the shape of the nanoparticle to a sphere.)

To explain the observed behavior, we need to consider two factors. First, the contribution of surface atoms in the RDF decreases rapidly when the particle size increases, as the RDF is averaged over all the atoms. Second, the EXAFS signal is sensitive to atoms up to 10 Å from the photoabsorbing atom (this is visually represented by a spherical probe of 20 Å diameter) when sampling different positions inside the nanoparticle. For a nanoparticle with a diameter of exactly 20 Å, all the photoabsorbing atoms experience an asymmetrical atomic environment, as the contribution of the core and surface atoms are both included in the same probe. For a particle with a diameter of 60 Å, though, where the radius of the spherical probe is smaller than the radius of

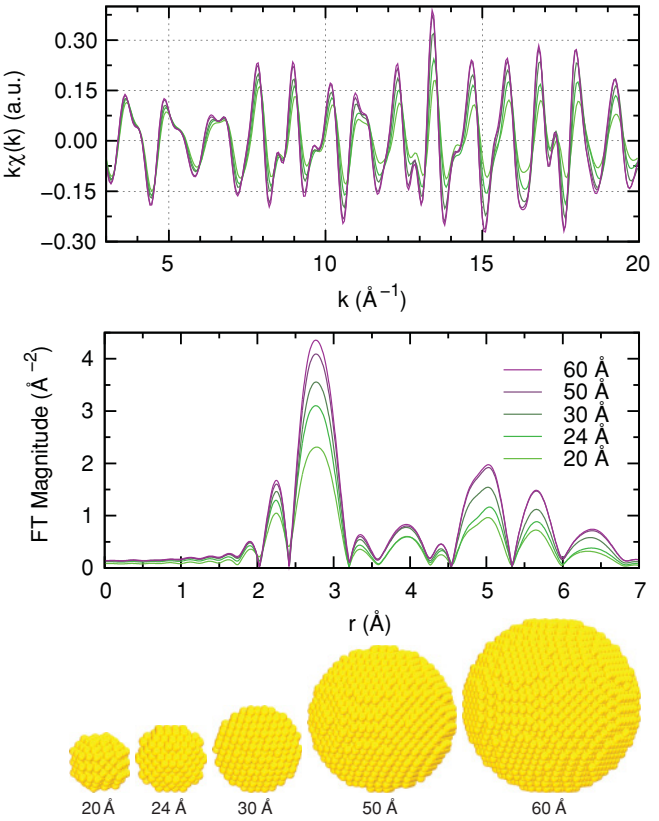

FIG. 6. (Color online) Simulated $k\chi(k)$ EXAFS spectra (top panel) and their Fourier transform (middle panel) as a function of nanoparticle size. The bottom panel shows a pictorial view of each gold nanoparticle.

the nanoparticle, different scattering regions can then be distinguished. Thus, a virtual sphere located in the inner region of the nanoparticle accounts only photoabsorbing atoms experiencing a symmetrical bulklike environment, while a spherical probe located at the surface scans a scattering region that is mainly asymmetrical. In the case of the largest nanoparticle, this asymmetrical region still represents 70% of its total volume.

The effect of temperature on the mean EXAFS spectrum of a gold nanoparticle with a diameter of 60 Å has also been studied. Figure 8 shows the spectra computed in a temperature

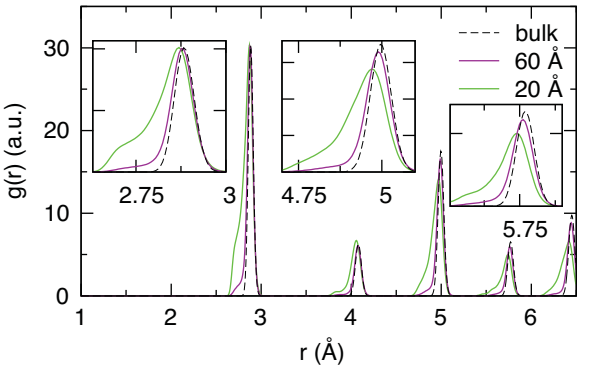

FIG. 7. (Color online) Radial distribution functions $g(r)$ extracted from MD trajectories at 20 K. The insets show the details of peaks 1, 3, and 4.

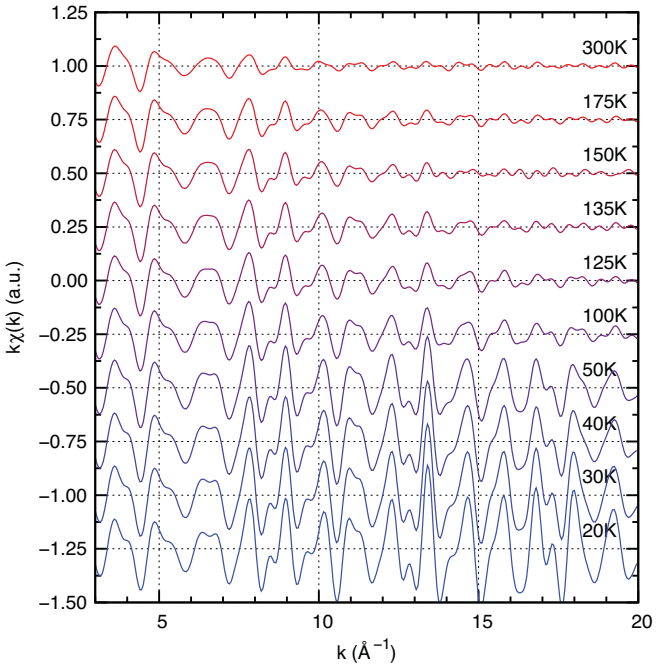

FIG. 8. (Color online) Effect of temperature on the simulated EXAFS spectra of a nanoparticle with a diameter of 60 Å.

range from 20 to 300 K. The increasing disorder of the nanoparticle structure caused by the increase in temperature causes a signal damping, leading eventually to a suppressed region in the $\chi(k)$ above 9 Å^{-1} at 300 K.

When comparing the mean EXAFS spectra of gold nanoparticles with a diameter of 24 and 50 Å with the experimentally determined spectra of nanoparticles with diameters of 24 ± 8 Å and 50 ± 7 Å, an underestimation of the bond lengths is observed in our MD simulations. To correct this error, we have scaled the structural models obtained from the MD snapshots by a numerical factor corresponding to the mean ratio between the experimental and the simulated bond lengths at 20 K. From the values reported in Table I, scaling factors of 0.9918 and 0.9971 were calculated to represent the spectroscopic properties of the nanoparticles with diameters of 24 and 50 Å, respectively. Figure 9 shows the EXAFS spectra of a gold nanoparticle with a diameter of 24 Å at 20 and 300 K in k space, while Fig. 11 shows the EXAFS spectra in r space at 20 K. As can be observed, a very good agreement is found between the simulated spectra and the experimental data. In particular, the phase and the shape of the oscillations are correctly reproduced from $k = 3$ to $k = 20$. The thermal damping of the EXAFS signal at the experimentally determined temperatures is not reproduced correctly in our calculations. We have found that the simulated mean EXAFS spectrum at 20 K has oscillations far too intense compared to the corresponding experimental spectrum, while the damping of the simulated mean EXAFS spectrum at 300 K is overestimated compared to the experimental spectrum. The best agreement between the simulated mean EXAFS spectra and their experimental counterparts at 20 and 300 K is found using MD trajectories at 60 and 150 K, respectively. We have investigated the origin of this discrepancy by carrying out MD simulations of the Au_{429} nanoparticle at 20 and 300 K with a different

TABLE I. Comparison between the shell distances (Å) for two gold nanoparticles at 20 K. Experimental values from Ref. 6. Calculated values from the radial distribution functions of Au_{429} (24 Å) and Au_{3925} (50 Å) at 20 K.

Au 24 ± 8 Å	R_1	R_2	R_3	R_4
Expt.	2.847(2)	4.026(8)	4.931(6)	5.694(6)
Calc.	2.867	4.062	4.974	5.742
Au 50 ± 7 Å	R_1	R_2	R_3	R_4
Expt.	2.876(2)	4.061(8)	4.975(6)	5.745(6)
Calc.	2.879	4.076	4.989	5.760

force field, in this instance, the Sutton-Chen potential.[26,27] We found that the mean EXAFS spectra obtained from these MD calculations are practically coincident with the mean EXAFS spectra previously computed.

Similar observations were made for the EXAFS spectra of a gold nanoparticle with a diameter of 50 Å at 20 and 300 K in k space and r space Figs. 10 and 11). However, for this system, there is a better agreement between the simulated and the experimental EXAFS spectra at 300 K, as the bigger size of the nanoparticle results in more intense oscillations of the EXAFS signal at high k values.

In summary, our results indicate that the unique features in the EXAFS spectra of gold nanoparticles arise mainly from the asymmetric scattering region, which is dominant in nanoparticles with diameters ranging from 20 to 60 Å. Furthermore, the discrepancies between the calculated and experimental

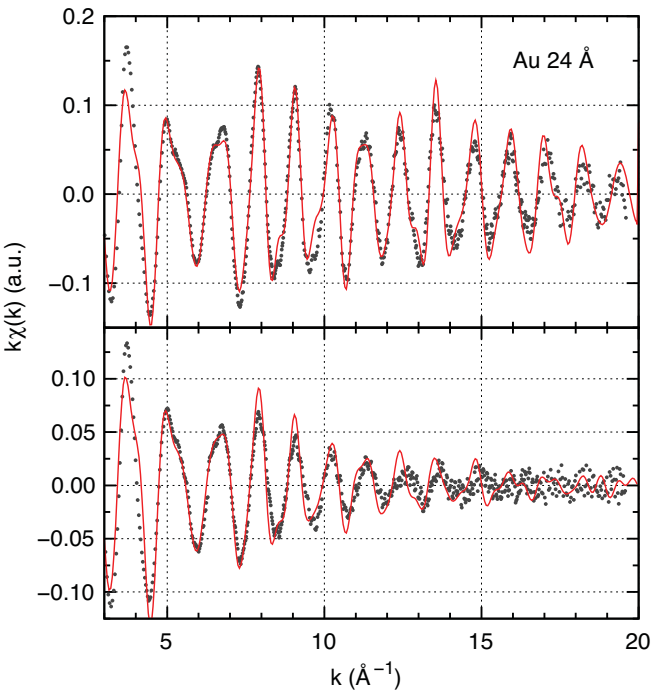

FIG. 9. (Color online) Experimental (dotted line) Au L_3-edge EXAFS spectra of a gold nanoparticle with a diameter of 24 Å, measured at 20 K (top panel) and 300 K (bottom panel). The theoretical spectra (solid line) have been obtained by averaging several structures obtained from MD simulations carried out at 60 K (top panel) and 150 K (bottom panel).

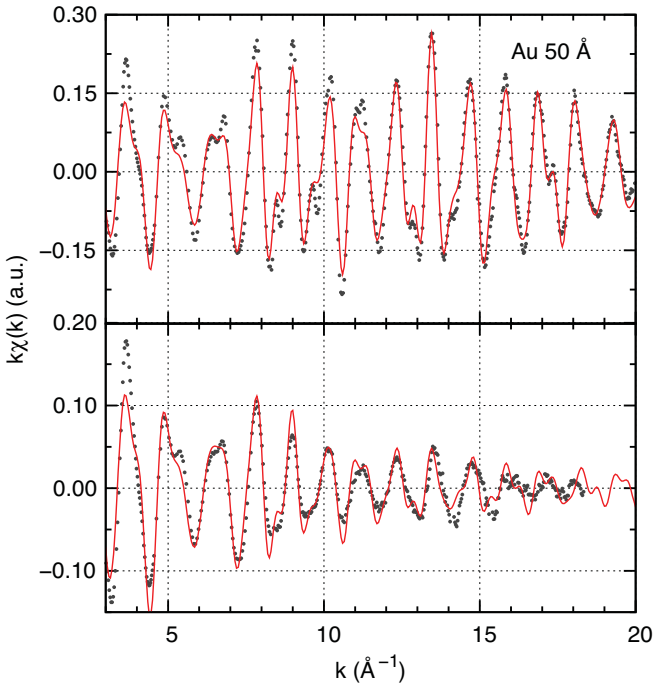

FIG. 10. (Color online) Experimental (dotted line) Au L_3-edge EXAFS spectra of a gold nanoparticle with a diameter of 50 Å, measured at 20 K (top panel) and 300 K (bottom panel). The theoretical spectra (solid line) have been obtained by averaging several structures obtained from MD simulations carried out at 40 K (top panel) and 150 K (bottom panel).

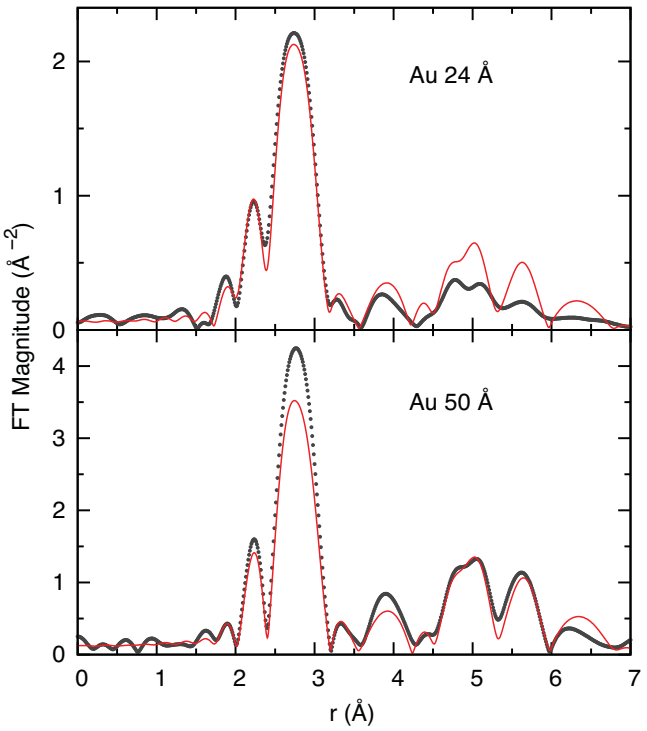

FIG. 11. (Color online) Experimental (dotted line) Au L_3-edge EXAFS spectra in r space of gold nanoparticles with a diameter of 24 Å (top panel) and 50 Å (bottom panel) at 20 K. The theoretical spectra (solid line) have been obtained by averaging several structures obtained from MD simulations carried out at 60 K (top panel) and 40 K (bottom panel).

EXAFS spectra can be attributed to the structural models of gold nanoparticles derived from the MD simulations. In particular, we have found that, in our models, the effect of surface compression is underestimated and it results in Au–Au bond lengths longer than the experimentally determined ones. This effect is more apparent in small nanoparticles where the theoretical mean Au–Au bond lengths are, on average, 0.8% longer than the experimentally determined bond lengths, while, for large nanoparticles, this difference shrinks to 0.3%.

IV. DISCUSSION

The EXAFS simulations of gold nanoparticles that we have presented in this paper show a remarkable agreement with the experimentally determined EXAFS spectra, providing support for the structural models obtained from classical MD simulations. The simulation of EXAFS spectra provides also a route for assessing the quality of the MD simulations, both for structural properties and thermal dynamics. We have identified two main differences between the simulated and experimentally determined properties of gold nanoparticles.

First, the average bond lengths in our MD simulations were larger than those fitted from analysis of the experimental EXAFS data. The difference, however, is smaller than 1%. The effect of surface tension is responsible for the shortening of the bond lengths observed in Fig. 5, and indeed the contribution of surface atoms clearly has a detectable effect on the simulated EXAFS spectra, as shown in Fig. 4. From these findings, we conclude that, in our MD simulations, the underestimation of the surface tension arises either because the region affected by the surface tension is not as deep as observed experimentally[24] or because the Au–Au bond lengths at the surface are larger than expected (e.g., with respect to the models presented in Ref. 25).

Second, although the thermal damping in our EXAFS simulations steadily increases with the temperature (Fig. 8), it does not reproduce the signal damping of experimentally determined EXAFS spectra at 20 and 300 K. The MD simulations at 20 K show small vibrational motions, resulting in an underestimation of the thermal damping. This effect is likely due to the fact that the classical molecular dynamics simulations neither include zero-point motion nor can they be expected to represent the dynamical ensemble accurately as, at this low temperature, it is dominated by the phonon vibrations of a quantum system, as mentioned in Sec. II B. By using a higher temperature in our simulations, we can compensate for this deficiency and obtain surprisingly close agreement with experiment. On the other hand, the vibrations at 300 K are large enough to produce a thermal disorder greater than the experiment. A deeper potential well might reduce the amplitude of vibrations at high temperature and could also decrease the bond lengths at the surface, as the resulting forces acting on gold atoms will be stronger.

Better agreement between the computational modeling and the experimental data would have been possible if a more accurate potential energy surface of the gold nanoparticles was used. The current work has been based on a force-field-generated potential energy surface due to the prohibitive

computational cost that *ab initio* molecular dynamics would have for problems of this size and simulations of this time scale (Ref. 2, see Sec. 4.1). In our case, the approximation made by representing the atomic interactions with a classical force field still gives reliable results for the structural properties of gold nanoparticles, although the vibrational motion is not reproduced accurately. A technique that provides a fine tuning of a force field by altering the curvature and depth of its potential well could be a promising step forward for a better agreement between the simulated and experimental EXAFS spectra. Nevertheless, it is expected that significant improvements while using the force field could be achieved by reparametrization or an alternative functional form that is more suitable for nanoparticles, given that the Gupta potential and other commonly used many-body force fields for metallic systems have been developed with calculations for bulk systems in mind. Furthermore, there is a degree of uncertainly about the actual temperature of the nanoparticles in the experiment, which can also be a source of discrepancy with the simulations as well as the fact that, in the experiment, the nanoparticles are supported on an amorphous silica surface, while in the simulations they are treated as isolated.

We expect that the approach presented here can be used as a tool to aid the interpretation of EXAFS spectra of nanoparticles and, hence, improve the analysis and size and shape characterization by EXAFS of newly synthesized nanoparticles.

V. CONCLUSIONS

We have presented a computational approach for the simulation EXAFS spectra of nanoparticles directly from classical MD simulations. We have shown that the computational procedure implemented in this work is able to compute correctly the EXAFS spectra of gold nanoparticles. A good agreement is found between the simulated and experimental Au L_3-edge EXAFS spectra of gold nanoparticles with different sizes, providing evidence about the reliability of the structural properties obtained from the MD simulations of the reported nanoparticles. Signal damping induced by thermal effects is also reproduced, although a fine tuning of the MD simulations appears to be necessary in order to reproduce the correct degree of disorder in the simulated EXAFS spectra. Our approach, which is based on MD simulations, is general and can be applied to calculate EXAFS spectra of any kind of nanoparticle, provided a suitable force field is available and that the simulation time can adequately sample its conformational space. Alternatively, in order to overcome the limitations of a classical approach, *ab initio* MD simulations could be used at a much higher computational cost. We envisage that our approach will serve as a computational tool for the more reliable interpretation of EXAFS spectra and, hence, the characterization of nanoparticle samples.

ACKNOWLEDGMENTS

O.M.R. would like to acknowledge Dr. Fabiola Liscio and Dr. Carlo Meneghini for useful discussions in the preparation of this work. N.Z. would like to thank the Southampton Nanoforum for funding support. C.-K.S would like to thank the Royal Society for financial support. We would like to acknowledge access to the University of Southampton's Iridis3 supercomputer.

*c.skylaris@soton.ac.uk

[1] F. Baletto and R. Ferrando, Rev. Mod. Phys. **77**, 371 (2005).
[2] R. Ferrando, J. Jellinek, and R. L. Johnston, Chem. Rev. (Washington, DC, US) **108**, 845 (2008).
[3] F. W. Lytle, D. E. Sayers, and E. A. Stern, Phys. Rev. B **11**, 4825 (1975).
[4] P. A. O'Day, J. J. Rehr, S. I. Zabinsky, and G. E. Brown Jr., J. Am. Chem. Soc. **116**, 2938 (1994).
[5] M.-C. Daniel and D. Astruc, Chem. Rev. (Washington, DC, US) **104**, 293 (2004).
[6] T. Comaschi, A. Balerna, and S. Mobilio, Phys. Rev. B **77**, 075432 (2008).
[7] K. J. Klabunde, Y. X. Li, and B. J. Tan, Chem. Mater. **3**, 30 (1991).
[8] M. P. Casaletto, A. Longo, A. M. Venezia, A. Martorana, and A. Prestianni, Appl. Catal., A **302**, 309 (2006).
[9] C. Bealing, G. Fugallo, R. Martonak, and C. Molteni, Phys. Chem. Chem. Phys. **12**, 8542 (2010); **12**, 8550 (2010).
[10] P. J. Merkling, A. Muñoz-Páez, and E. S. Marcos, J. Am. Chem. Soc. **124**, 10911 (2002).
[11] O. M. Roscioni, P. D'Angelo, G. Chillemi, S. D. Longa, and M. Benfatto, J. Synchrotron Radiat. **12**, 75 (2005).
[12] P. D'Angelo, O. M. Roscioni, G. Chillemi, S. D. Longa, and M. Benfatto, J. Am. Chem. Soc. **128**, 1853 (2006).
[13] F. Carrera, F. Torrico, D. T. Richens, A. Muñoz-Páez, J. M. Martínez, and R. Rafael, J. Phys. Chem. B **111**, 8223 (2007).
[14] P. D'Angelo, V. Migliorati, G. Mancini, and G. Chillemi, J. Phys. Chem. A **112**, 11833 (2008).
[15] P. D'Angelo, A. Zitolo, V. Migliorati, G. Mancini, I. Persson, and G. Chillemi, Inorg. Chem. (Washington, DC, US) **48**, 10239 (2009).
[16] E. C. Beret, K. Provost, D. Müller, and E. S. Marcos, J. Phys. Chem. B **113**, 12343 (2009).
[17] R. P. Gupta, Phys. Rev. B **23**, 6265 (1981).
[18] F. Cleri and V. Rosato, Phys. Rev. B **48**, 22 (1993).
[19] W. Smith and T. R. Forester, J. Mol. Graphics **14**, 136 (1996).
[20] Accelrys, Materials Studio. Inc, Accelrys Software, 2001–2007.
[21] J. M. Soler, M. R. Beltrán, K. Michaelian, I. L. Garzón, P. Ordejón, D. Sánchez-Portal, and E. Artacho, Phys. Rev. B **61**, 5771 (2000).
[22] A. L. Ankudinov, B. Ravel, J. J. Rehr, and S. D. Conradson, Phys. Rev. B **58**, 7565 (1998).
[23] B. Ravel, J. Alloys Compd. **401**, 118 (2005).
[24] W. J. Huang, R. Sun, J. Tao, L. D. Menard, R. G. Nuzzo, and J. M. Zuo, Nat. Mater. **7**, 308 (2008).
[25] A. Yevick and A. I. Frenkel, Phys. Rev. B **81**, 115451 (2010).
[26] A. P. Sutton and J. Chen, Philos. Mag. Lett. **61**, 139 (1990).
[27] H. Rafii-Tabar and A. P. Sutton, Philos. Mag. Lett. **63**, 217 (1991).